Reconstitution of a minimal machinery capable of assembling periplasmic type IV pili

Vivianne J. Goosens[a,1], Andreas Busch[b,1], Michaella Georgiadou[a], Marta Castagnini[a], Katrina T. Forest[c], Gabriel Waksman[b], and Vladimir Pelicic[a,2]

[a]Medical Research Council Centre for Molecular Bacteriology and Infection, Imperial College London, London SW7 2AZ, United Kingdom; [b]Institute of Structural and Molecular Biology, University College London and Birkbeck College, London WC1E 7HX, United Kingdom; and [c]Department of Bacteriology, University of Wisconsin–Madison, Madison, WI 53706

Type IV pili (Tfp), which are key virulence factors in many bacterial pathogens, define a large group of multipurpose filamentous nanomachines widespread in Bacteria and Archaea. Tfp biogenesis is a complex multistep process, which relies on macromolecular assemblies composed of 15 conserved proteins in model gram-negative species. To improve our limited understanding of the molecular mechanisms of filament assembly, we have used a synthetic biology approach to reconstitute, in a nonnative heterologous host, a minimal machinery capable of building Tfp. Here we show that eight synthetic genes are sufficient to promote filament assembly and that the corresponding proteins form a macromolecular complex at the cytoplasmic membrane, which we have purified and characterized biochemically. Our results contribute to a better mechanistic understanding of the assembly of remarkable dynamic filaments nearly ubiquitous in prokaryotes.

type IV pili | type IV filamentous nanomachines | filament assembly | synthetic biology

Evolution has provided prokaryotes with sophisticated surface nanomachines that endow them with many functions instrumental to their ability to colonize most niches on Earth. Among these engineering marvels, type IV filamentous (Tff) nanomachines (1), of which type IV pili (Tfp) are the paradigm, are unique for two reasons. They are exceptionally (*i*) widespread, with genes encoding distinctive proteins found in virtually every prokaryotic genome, and (*ii*) multipurpose, associated with functions as diverse as adhesion, motility, protein secretion, DNA uptake, electric conductance, and so forth (1). Much of this broad distribution and multifunctionality is due to Tfp (1).

All Tff nanomachines share multiple components and are thought to use common basic operating principles. They have at their core a filament, which can be long or short and is a polymeric assembly of a protein named pilin, PilE in our model Tfp-expressing species *Neisseria meningitidis* (meningococcal nomenclature will be used here). Type IV pilins are produced as prepilins with a distinctive N-terminal class III signal peptide (2), consisting of a short hydrophilic leader peptide followed by a stretch of 21 hydrophobic residues, always forming an extended α-helix (3). This signal peptide is first recognized by the Sec machinery (4, 5), which translocates prepilins across the cytoplasmic membrane, where they remain embedded as bitopic proteins. The leader peptide is then cleaved by an integral membrane aspartic protease (6, 7), the prepilin peptidase PilD. This processing, which does not require other Pil proteins (8), is a prerequisite for polymerization of pilins into filaments. Filaments are helical polymers in which the pilins' extended N-terminal α-helices are buried within the filament core, almost parallel to its long axis (9). Finally, in gram-negative Tfp-expressing bacteria, filaments cross the outer membrane through a pore formed by the secretin PilQ (10).

The molecular mechanisms of filament assembly remain poorly understood. However, there is consensus that assembly occurs at the cytoplasmic membrane and requires energy, which is generated by PilF, a cytoplasmic ATPase (11–13). This energy is transmitted via an ill-defined membrane-embedded assembly subcomplex to the processed pilins, which are thereby extruded from the lipid bilayer and polymerized into filaments. Filament assembly has been best-studied in gram-negative species expressing retractable Tfp, where piliation relies on 15 highly conserved proteins (1) (PilC, PilD, PilE, PilF, PilG, PilH, PilI, PilJ, PilK, PilM, PilN, PilO, PilP, PilQ, and PilW). Genetic studies have shown that seven of these proteins are not involved in filament assembly per se, because piliation can be restored in the corresponding mutants by a second mutation in *pilT*, which encodes an ATPase powering pilus retraction/disassembly (14). As confirmed in different species, these seven proteins are the outer-membrane component PilC (15, 16), the four pilin-like proteins (PilH, PilI, PilJ, and PilK) (16–18), the secretin PilQ (16, 19), and the secretin-associated lipoprotein PilW (20, 21). Interestingly, in the *pilQpilT* double mutant, filaments remain trapped in the periplasm (16, 19), showing that filament assembly can be genetically uncoupled from their emergence on the cell surface. As a corollary, when piliation was not restored in a double mutant, this was viewed as indirect evidence that the corresponding Pil protein might be involved in filament assembly. Although different studies agree that PilD, PilE, and PilF fall in this class (16, 19), conflicting results have been obtained for PilG, PilM, PilN, PilO, and PilP. In *N. meningitidis*, PilM, PilN, PilO, and PilP were deemed essential for filament assembly although the integral membrane protein (PilG) was not (16), whereas in *Pseudomonas aeruginosa* it was the opposite scenario (22). As a result, the exact role of these five proteins is unclear,

Significance

Type IV pili (Tfp) define a group of multipurpose filamentous nanomachines widespread in Bacteria and Archaea. Tfp biogenesis is a complex process relying on machines composed of up to 15 conserved proteins. Here, to improve our limited understanding of the molecular mechanisms of filament assembly, we have reconstituted in a nonpiliated heterologous host a minimal machinery capable of building Tfp. We show that eight proteins are sufficient to promote filament assembly and that they form a macromolecular complex at the cytoplasmic membrane, which we have purified and characterized biochemically. Our results contribute to a better mechanistic understanding of the functioning of filamentous nanomachines nearly ubiquitous in prokaryotes.

but there is ample evidence that they establish multiple binary/ternary interactions at the cytoplasmic membrane (23–33). Moreover, in a recent study in *Myxococcus xanthus*, in which the entire Tfp machinery was visualized by cryoelectron tomography (34), it was shown that these five proteins form a series of interconnected layers spanning the cytoplasmic membrane, which is a priori compatible with a role in filament assembly.

Although the above mutational studies defining Pil components essential for Tfp assembly have provided a useful blueprint for subsequent experiments, they are inherently limited by their negative readout (absence of piliation in a *pilT* mutant background) and the contrasting findings in two closely related systems (*N. meningitidis* and *P. aeruginosa*). Here, we have directly defined the proteins required for Tfp assembly by using a previously unexplored synthetic biology approach. By identifying the minimal set of Pil proteins capable of assembling Tfp in a heterologous host in which they are not natively produced and characterizing biochemically the macromolecular complexes these proteins form, we provide novel insights into a fundamental but poorly understood phenomenon.

Results

Engineering Large Synthetic Operons Encoding Proteins Involved in Tfp Assembly.
Reconstituting a minimal machinery capable of assembling Tfp is challenging because of (*i*) the large number of genes required, and (*ii*) the fact that these genes are scattered over many genomic loci. To overcome these challenges, *pil* genes from the sequenced *N. meningitidis* 8013 strain (35), codon-optimized for expression in *Escherichia coli*, were synthesized

for each meningococcal protein potentially involved in Tfp assembly (PilD, PilE, PilF, PilG, PilM, PilN, PilO, and PilP). To engineer large artificial operons with these synthetic genes, we used an iterative cloning approach (36). Genes were combined into operons of increasing size, where each gene was preceded by a ribosome-binding site (RBS) and the expression of the entire operon was driven by a T7 promoter (Fig. S1). First, to test experimentally the two contrasting models for Tfp assembly, we engineered *pilDFGE* and *pilDFMNOPE* operons (abbreviated as DFGE or DFMNOPE) (Fig. 1*A*). However, because toxicity and plasmid instability were observed in a variety of BL21-based expression strains, we subcloned these operons into pBAD18 under a tighter arabinose-inducible promoter (37). These pBAD18-derived plasmids were stable and did not significantly affect bacterial growth. All of the Pil components included in these operons were expressed, as tested by immunoblotting using specific antibodies (Fig. 1*B*). Because we have been unable to generate a good anti-PilD antibody, we confirmed the presence of a functional prepilin peptidase by showing that PilE was processed only when *pilD* was present. In the absence of PilD (first lane), PilE has a slightly larger molecular weight than in bacteria where PilD is present (lanes 2 to 7) (Fig. 1*B*). Our attempts to construct operons encoding all of the above eight Pil components were thwarted by plasmid instability. We therefore used an alternative cloning strategy to create pBAD18 derivatives expressing these eight genes from two different promoters (Fig. 1*A*). The DFGE and DFMNOPE operons were subcloned into pBAD18 under a constitutive σ70 promoter, which was mapped using 5′ RACE (Fig. S2). The resulting plasmids were then used to subclone the remaining *pil* gene(s) under the arabinose-inducible promoter, yielding MNOP[DFGE] and
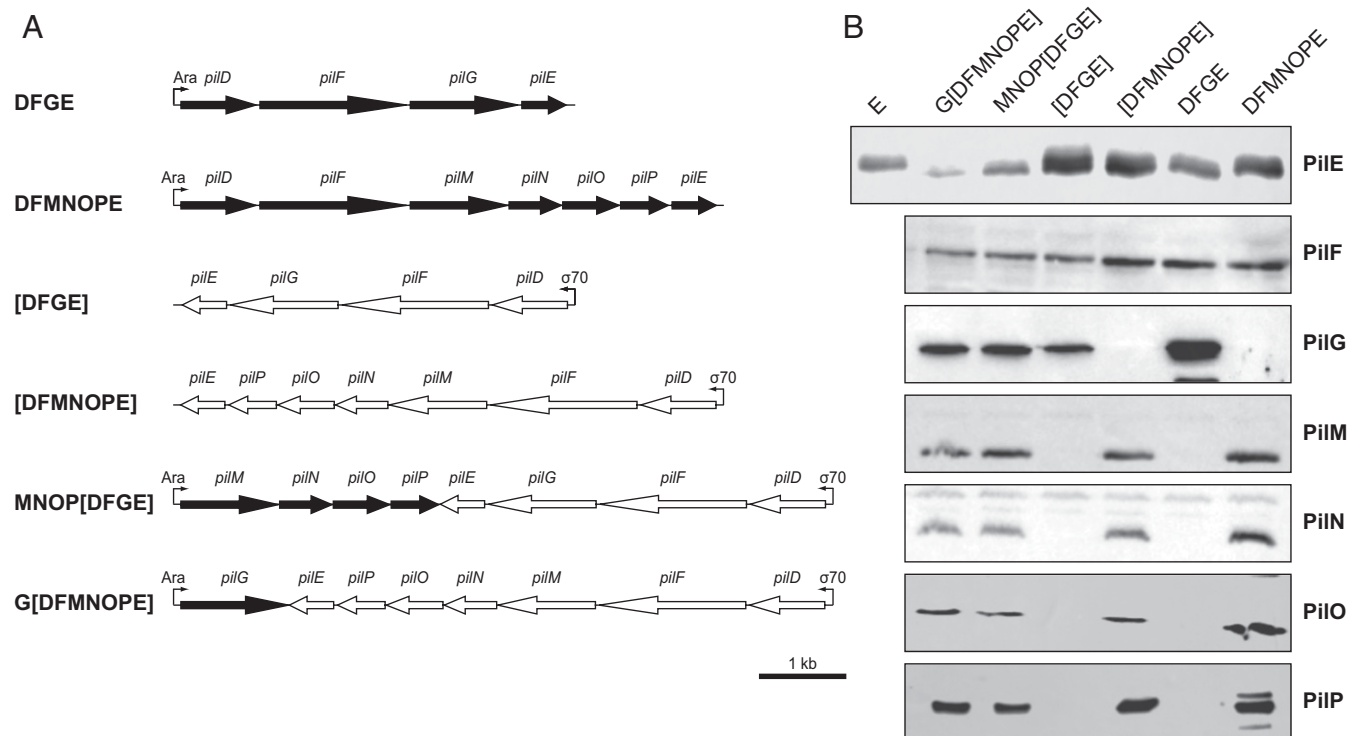

Fig. 1. Engineering large operons composed of synthetic meningococcal genes optimized for expression in *E. coli*, which encode proteins involved in Tfp assembly. (*A*) Gene organization of *pil* operons generated in pBAD18 in this study. Expression of genes in black is driven by an arabinose-inducible promoter (Ara). Expression of genes in white, indicated within brackets, is driven by a constitutive σ70 promoter (σ70). All of the genes are drawn to scale. (Scale bar, 1 kb.) (*B*) Immunoblot analysis of the production of Pil proteins from various constructs. Whole-cell protein extracts of *E. coli* TOP10 transformed with the various constructs (indicated above each lane) were probed using specific anti-Pil antibodies (indicated on the right of each immunoblot). Because no antibody is available against PilD, we confirmed the presence of a functional prepilin peptidase by showing that the pilin detected (*Top*) in a strain expressing only PilE (lane 1) has a slightly larger molecular weight than the pilin detected in the bacteria where PilD is present (lanes 2 to 7). Bacterial cultures were equalized based on OD_{600} readings, and equivalent amounts of cells were loaded in each lane.

G[DFMNOPE] constructs (genes within brackets are those whose expression is driven by σ70). The final plasmids were stable, did not significantly affect bacterial growth, and led to the expression of all of the Pil components as tested by immunoblotting (Fig. 1B).

Pil Proteins Form Membrane-Embedded Macromolecular Assemblies, Which Can Be Purified to Homogeneity. To promote Tfp assembly, the Pil proteins expressed in *E. coli* must interact to form a macromolecular complex at the cytoplasmic membrane. Therefore, to test complex formation/stability and unravel protein–protein interactions between the PilF, PilG, PilM, PilN, PilO, and PilP components, we added a *Strep* tag to either PilO or PilP (indicated as P_{Strep} or O_{Strep}) and purified under native conditions the complexes formed by various protein combinations. Notably, when the *pilMNOP*$_{Strep}$ operon was expressed, we could purify a native PilMNOP$_{Strep}$ complex solubilized in *n*-dodecyl β-D-maltoside (β-DDM) using a combination of affinity chromatography and size-exclusion chromatography (SEC). As shown in Fig. 2, PilMNOP$_{Strep}$, which is stable throughout the purification process, eluted as a single, symmetric peak during SEC. The purified complex consisted of the four PilM, PilN, PilO, and PilP$_{Strep}$ components as assessed by Coomassie staining after SDS/PAGE (Fig. 2) and immunoblotting (Fig. S3). A MALDI-TOF MS analysis of the purified complex in solution confirmed that the four Pil components were intact (Fig. S4). Using SEC coupled with in-line multiangle light scattering (SEC-MALS), PilMNOP$_{Strep}$ was found to be a homogeneous and monodisperse sample with an estimated molecular weight of 132.7 ± 1.6 kDa (Table S1). This value is reasonably close to the theoretical molecular weight of a heterotetramer (108 kDa), suggesting that the purified PilMNOP$_{Strep}$ complex consists of one copy of each protein (1:1:1:1 stoichiometry). Next, we tested whether these four components are all necessary for complex formation and/or stability by generating alternative constructs with *pilMNO*$_{Strep}$ and *pilNOP*$_{Strep}$ operons. Whereas PilNOP$_{Strep}$ could be purified as a stable and homogeneous complex (Fig. 3A), indicating that PilM is dispensable for complex formation/stability, the PilMNO$_{Strep}$ complex eluted in several peaks and the proteins in the different fractions tended to aggregate after purification (Fig. S5), indicating that PilP is important for PilMNOP$_{Strep}$ stability. Strikingly, a *Strep*-tagged 9.8-kDa truncated version of PilP (named PilP$_{NT-Strep}$), consisting only of the N-terminal 77 residues previously shown to interact with

PilNO (29), was sufficient to restore stability and homogeneity to the PilMNOP complex (Fig. 3B). Using SEC-MALS, PilNOP$_{Strep}$ was found to be a homogeneous and monodisperse sample (Table S1). Intriguingly, the estimated molecular weight of PilNOP$_{Strep}$, 214.9 ± 9.2 kDa, was much larger than the theoretical molecular weight of a heterotrimer (66.7 kDa) and even larger than the molecular weight measured for PilMNOP$_{Strep}$. This finding, which is consistent with the lower retention volumes for PilNOP$_{Strep}$ compared with PilMNOP$_{Strep}$, suggests that PilNOP$_{Strep}$ adopts a different 3:3:3 stoichiometry in the absence of PilM.

We next assessed whether the other two putative filament assembly components (PilF and PilG) form a complex with PilMNOP. Whereas coexpression of the six genes failed to yield amounts of proteins sufficient for analysis, *pilF*$_{His}$*MNOP*$_{Strep}$ and *pilG*$_{His}$*MNOP*$_{Strep}$, where PilF and PilG have C-terminally fused His tags, produced complexes consisting of all five Pil components. Both PilF$_{His}$MNOP$_{Strep}$ (Fig. 4A) and PilG$_{His}$MNOP$_{Strep}$ (Fig. 4B) are stable and homogeneous complexes, which eluted during SEC as single, symmetric peaks. The presence of all complex components was confirmed by immunoblotting (Fig. S6). To determine whether PilF and PilG could interact with the stable PilNOP complex, we coexpressed *pilF*$_{His}$ or *pilG*$_{His}$ with *pilNOP*$_{Strep}$. We found that PilF$_{His}$ could not be pulled down with the PilNOP$_{Strep}$ complex (Fig. S7A), suggesting that PilM is the likely interaction partner of PilF. Similarly, PilG$_{His}$ did not form a stable complex with PilNOP$_{Strep}$. The protein complexes that were pulled down eluted in several peaks in which no PilG$_{His}$ was detectable by Coomassie staining after SDS/PAGE (Fig. S7B), although the protein (probably minute amounts) could be detected by immunoblotting in the higher molecular weight peaks. These findings show that PilM is important for the stability of PilG within the PilGMNOP complex.

Taken together, these results show that the Pil components predicted to play a role in Tfp assembly form stable membrane macromolecular complexes, which could be purified in native fashion.

Addressing the PilG "Paradox" in *N. meningitidis*. It has been reported in *N. meningitidis* 8013 that piliation is restored in a *pilGpilT* mutant (16), which is in stark contrast with subsequent results in *P. aeruginosa* (22) and the central position of PilG in subtomograms of the *M. xanthus* Tfp machinery (34). The biochemical evidence above that PilG forms a complex with PilMNOP prompted us to revisit PilG's role in *N. meningitidis*. First, because the anti-PilG antibody was not available during our original study, we determined whether the *pilG* transposon insertion (Tn) mutant that was used then (called *pilG1* hereafter), which has a *mariner* minitransposon inserted close to the beginning of this gene (Fig. 5A), disrupts protein production. As can be seen in Fig. 5B, this is indeed the case, because no PilG could be detected by immunoblotting in whole-cell protein extract from the *pilG1* mutant. Then, as assessed by immunofluorescence (IF) microscopy, using the 20D9 monoclonal antibody that is highly sensitive and specific for strain 8013 Tfp (38), we confirmed earlier findings (16) that the *pilG1* mutant is nonpiliated and that piliation is restored in a *pilG1pilT* double mutant, which is heavily piliated (Fig. 5C). To determine whether different *pilG* mutations would yield similar results or not, we constructed two additional double mutants using either a *pilG2* Tn mutant with an insertion closer to the middle of the gene or a Δ*pilG* mutant in which the gene was cleanly deleted (27) (Fig. 5A). Strikingly, although both these mutations abolish PilG production (Fig. 5B), the *pilG2pilT* and Δ*pilG*Δ*pilT* mutants behaved differently from *pilG1pilT* because they were nonpiliated (Fig. 5C). Not a single filament could be detected by IF microscopy in the *pilG2pilT* and Δ*pilG*Δ*pilT* mutants. Together, these results show that although the nonpiliated phenotype in the *N. meningitidis pilG1* mutant can indeed be suppressed by a second mutation in *pilT*, this is dependent on the nature of this *pilG* mutation. Therefore, because
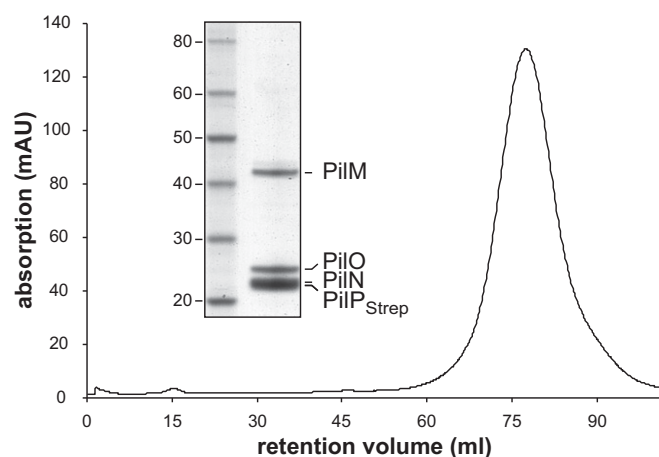

Fig. 2. PilMNOP proteins form a stable membrane complex when expressed in *E. coli*, which can be purified to homogeneity. SEC profile of PilMNOP$_{Strep}$ on a Superose 6 XK 16/70 column. mAU, milli absorbance unit. (*Inset*) SDS/PAGE/Coomassie analysis of the purified complex. A molecular weight marker was run in the first lane. Molecular weights are indicated in kDa. The molecular weights for the individual proteins are PilM, 41.4 kDa; PilN, 22.2 kDa; PilO, 23.3 kDa; and PilP$_{Strep}$, 21.3 kDa.
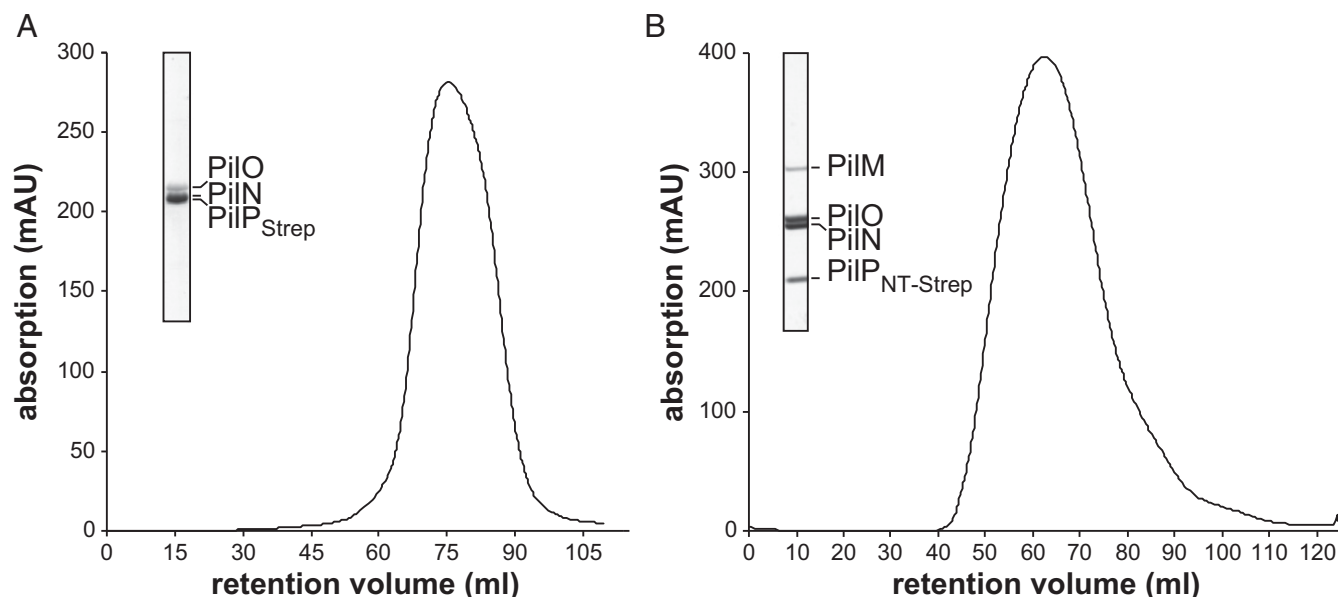
Fig. 3. PilM is dispensable for the stability of the PilMNOP complex, whereas PilP is essential via its unstructured N-terminal domain. (*A*) PilNOP$_{Strep}$ is a stable membrane complex, which can be purified to homogeneity. SEC profile of PilNOP$_{Strep}$ on a Superose 6 XK 16/70 column. (*A*, *Inset*) SDS/PAGE/Coomassie analysis of the purified complex. (*B*) PilMNOP$_{NT-Strep}$, in which PilP has been truncated down to its predicted unstructured N-terminal domain, is a stable membrane complex, which can be purified to homogeneity. SEC profile of PilMNOP$_{NT-Strep}$ on a Superose 6 10/300 GL column. (*B*, *Inset*) SDS/PAGE/Coomassie analysis of the purified complex. The molecular weight for PilP$_{NT-Strep}$ is 9.8 kDa.

no filaments are restored when *pilG* is cleanly deleted, PilG is likely to be involved in pilus assembly in *N. meningitidis*.

Eight Proteins Are Sufficient to Assemble Tfp. Using our monoclonal 20D9 anti-Tfp antibody, which specifically and efficiently recognizes filaments from strain 8013 (38), we assessed by IF microscopy whether the expression of any of the above *pil* operons would promote filament assembly in *E. coli*. An important caveat is that because no *pilQ* was included in our constructs, potential Tfp were expected to be trapped in the periplasm, much like

the filaments in a meningococcal double *pilQpilT* mutant (16). Bacteria were therefore submitted to an osmotic shock treatment before IF microscopy, as previously done for *N. meningitidis pilQpilT* (16). We first tested the two models for Tfp assembly preexisting this study, PilDEFG vs. PilDEFMNOP (16, 22). No filaments were detected when the [DFGE] or [DFMNOPE] operons were expressed in *E. coli* (Fig. 6 *A* and *B*). This shows that (*i*) neither of these two operons promotes Tfp assembly, and (*ii*) filament assembly does not occur spontaneously, confirming previous findings that the anti-Tfp monoclonal antibody shows
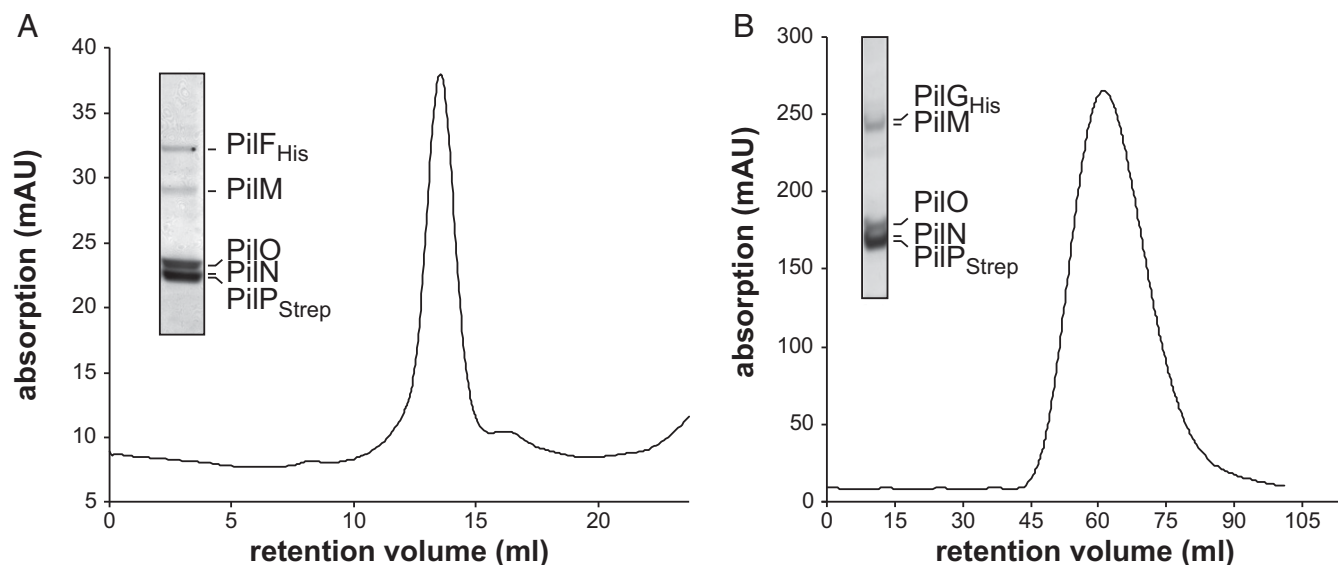
Fig. 4. Tfp assembly proteins PilG and PilF interact with PilMNOP, forming stable membrane complexes, which can be purified to homogeneity. (*A*) SEC profile of PilF$_{His}$MNOP$_{Strep}$ on a Superose 6 10/300 GL column. (*A*, *Inset*) SDS/PAGE/Coomassie analysis of the purified complex. The molecular weight for PilF$_{His}$ is 63.2 kDa. (*B*) SEC profile of PilG$_{His}$MNOP$_{Strep}$ on a Superose 6 XK 16/70 column. (*B*, *Inset*) SDS/PAGE/Coomassie analysis of the purified complex. The molecular weight for PilG$_{His}$ is 46.5 kDa.
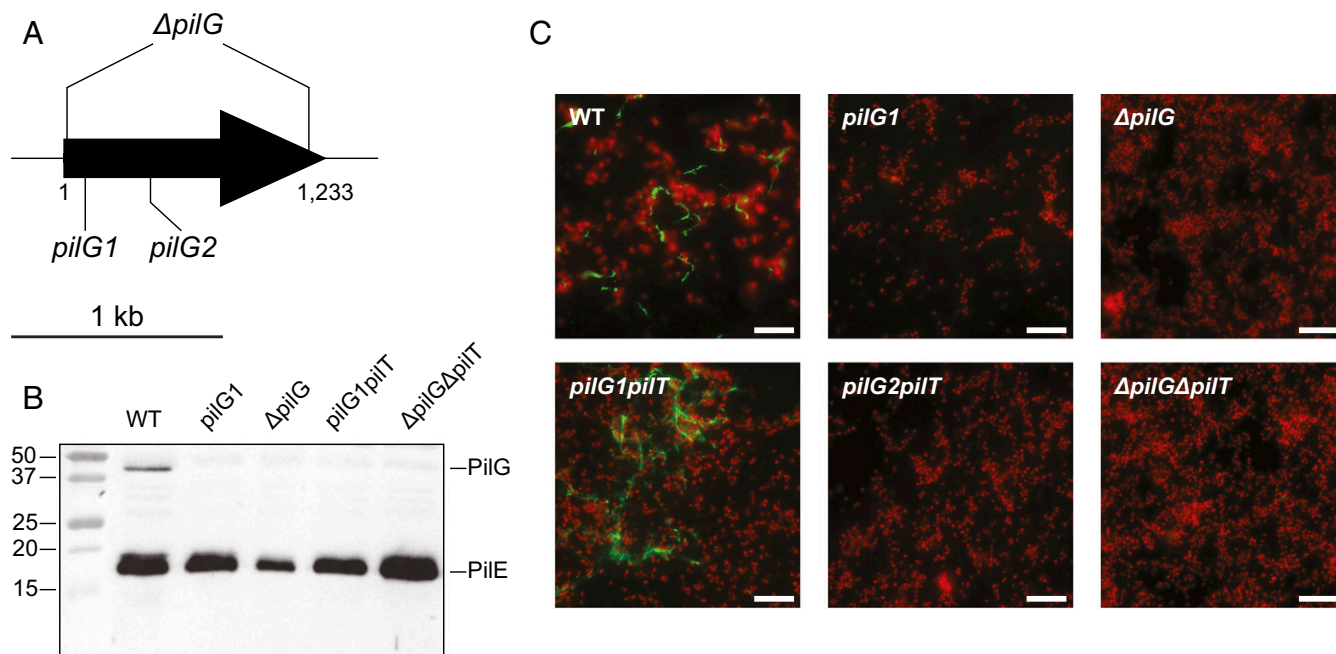
Fig. 5. PilG is important for Tfp assembly in *N. meningitidis*. (*A*) Schematic representation of *pilG* from *N. meningitidis* 8013 and the different mutations analyzed in this study. *pilG1* and *pilG2* are Tn insertion mutants, whereas Δ*pilG* is a mutant in which the gene has been deleted and replaced with a cassette encoding kanamycin resistance. Picture is drawn to scale. (Scale bar, 1 kb.) (*B*) Immunoblot analysis of PilG production in the different mutants. Double mutants include either a *pilT* mutant with an inserted cassette encoding erythromycin resistance or a Δ*pilT* deletion mutant in which the gene has been deleted and replaced by a cassette encoding erythromycin resistance. Whole-cell meningococcal protein extracts were probed using anti-PilG and anti-PilE (as a positive control) antibodies together. Protein extracts were quantified and equalized, and equivalent amounts of total proteins were loaded in each lane. Molecular weights are indicated in kDa. (*C*) Piliation as assessed by IF microscopy in the various *N. meningitidis pilG* mutants. The WT strain was included as a positive control. Tfp (green) were labeled with a monoclonal antibody specific for strain 8013 filaments and a secondary antibody coupled to Alexa Fluor 488, whereas bacteria (red) were stained with DAPI. All the pictures were taken at the same magnification. (Scale bars, 10 μm.)

specificity for assembled Tfp (38). Instead, with both of the above gene combinations, we saw green spots/foci localized on the bacterial cells (Fig. 6 *A* and *B*). Because we showed above that all of the corresponding proteins are expressed and form membrane-embedded macromolecular complexes, the absence of piliation suggests that none of the PilDEFG and PilDEFMNOP subsets of proteins is sufficient to promote Tfp assembly. Therefore, because we found in this study that PilG is essential for filament assembly in *N. meningitidis* and that it interacts with PilMNOP to form a PilGMNOP complex, we tested whether *E. coli* strains transformed with the MNOP[DFGE] (Fig. 6 *C* and *E*) and G[DFMNOPE] (Fig. 6 *D* and *F*) constructs would be capable of producing Tfp. Strikingly, micrometer-long filaments (a length similar to native meningococcal Tfp) were readily and reproducibly detected. Filaments were seen with both operons, in which the genes are in different orders and expressed from different promoters, confirming that the eight proteins are sufficient to promote filament assembly. Filaments were not detected when the bacteria were not osmotically shocked, confirming that they were originally trapped in the periplasm (Fig. 6 *G* and *H*). Taken together, these results show that eight proteins (PilD, PilE, PilF, PilG, PilM, PilN, PilO, and PilP) are sufficient to promote Tfp assembly, indicating that these proteins form the minimal machinery capable of polymerizing PilE into filaments.

Discussion

Tff nanomachines are nearly ubiquitous in prokaryotes and have been studied for decades. However, our understanding of the molecular mechanism(s) leading to the assembly of filaments composed of type IV pilins remains limited. This is in part due to the complexity of the protein machinery involved, with as many as 15 highly conserved proteins involved in gram-negative model species (1). In addition, the integral membrane nature of these

protein complexes has hindered biochemical and structural studies. Here we have used a synthetic biology approach to reconstitute in *E. coli* a minimal machinery capable of assembling Tfp, which we characterized in depth biochemically. This led to the notable findings discussed below.

Our genetic evidence that the "platform" protein PilG is involved in filament assembly is important, as it solves the *Neisseria* PilG paradox. This finding is now consistent with PilG's (*i*) presence in all Tff nanomachines (1), (*ii*) central position in the Tfp machinery of *M. xanthus* (34), and (*iii*) role in Tfp assembly in *P. aeruginosa* (22). Nevertheless, the piliated phenotype of the *pilG1pilT* mutant is intriguing and unique to the *pilG1* mutation, where a Tn is inserted early in the gene after the first 100 bp. Although speculative, the most likely scenario is that a truncated PilG protein is still produced in this mutant. Although this putative truncated protein, which we could not detect by immunoblotting, is unable to promote piliation in an otherwise WT genetic background, it might be partially active and capable of promoting filament assembly in a *pilT* mutant background. The N terminus of PilG is therefore likely to be dispensable for filament assembly, and its role could be to promote piliation by controlling PilT-mediated pilus retraction. This scenario is consistent with the observation that the N terminus is the least conserved portion in PilG orthologs.

A key finding in this study is that a minimal machinery capable of assembling Tfp can be reconstituted in *E. coli* by coexpressing only 8 of the 15 highly conserved Pil proteins in species expressing retractable Tfp. Our results indicate that the 7 Pil proteins acting after pilus assembly (PilC, PilH, PilI, PilJ, PilK, PilQ, and PilW) are dispensable en bloc for filament assembly. Because PilD, PilE, and PilF roles are known, our results suggest that 5 components (PilG, PilM, PilN, PilO, and PilP) form the macromolecular complex
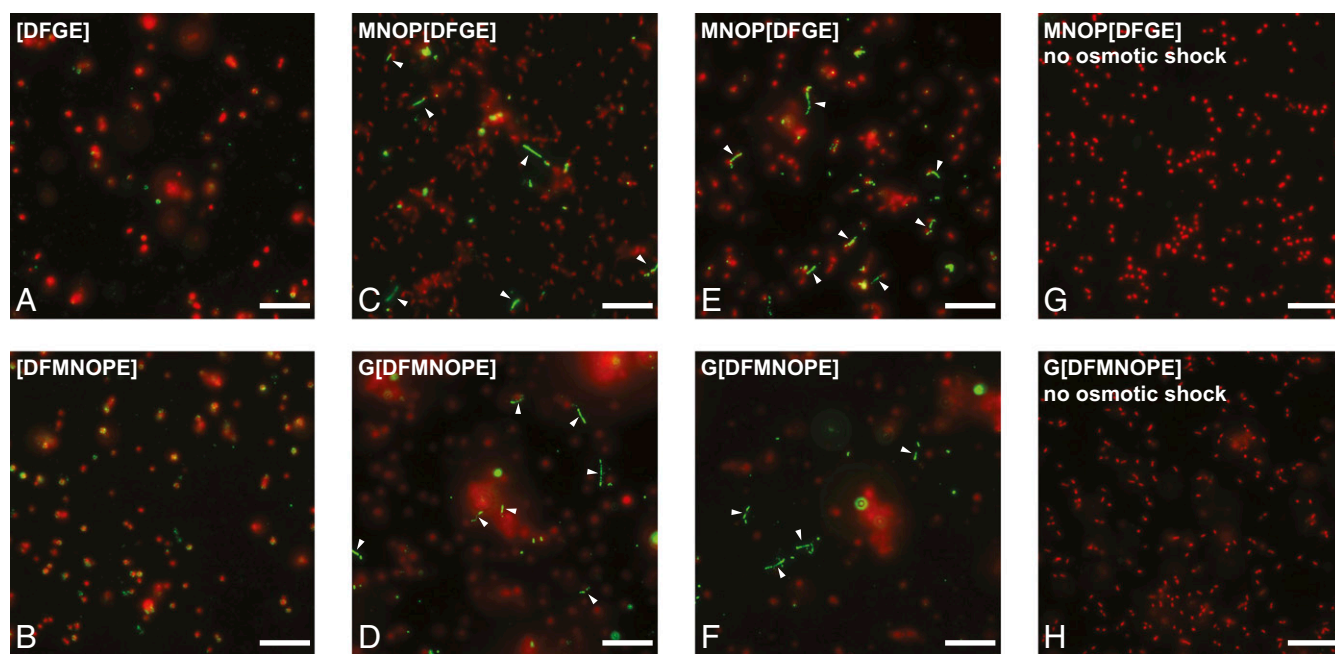
Fig. 6. Eight Pil proteins (PilD, PilE, PilF, PilG, PilM, PilN, PilO, and PilP) are necessary and sufficient to promote Tfp assembly. The presence of filaments in *E. coli* TOP10 transformed with various *pil* constructs (indicated in the upper left corner of each panel) was assessed by IF microscopy. Tfp (green) were labeled with a monoclonal antibody highly specific for strain 8013 filaments and a secondary antibody coupled to Alexa Fluor 488, whereas bacteria (red) were stained with DAPI. Except where indicated (*G* and *H*), the presence of filaments was assessed after the bacteria were submitted to an osmotic shock treatment to release their periplasmic content (*A–F*). For those *pil* combinations that led to Tfp assembly, MNOP[DFGE] (*C* and *E*) and G[DFMNOPE] (*D* and *F*), two different experiments are shown. Long filaments are indicated by white arrowheads. All the pictures were taken at the same magnification. (Scale bars, 10 μm.)

involved in filament assembly. Therefore, both preexisting models for Tfp assembly (16, 22) were partially correct, because both PilG and PilMNOP are required. However, in the presence of PilDFGE or PilDFMNOPE only, foci but not filaments were detected, which suggests an abortive filament assembly process. The PilMNOP subcomplex is therefore not merely an "alignment subcomplex" responsible for aligning the filament assembly machinery with the secretin pore in the outer membrane (29). Instead, it is an integral and key part of the assembly machinery itself. This is supported by the presence of PilM and PilN orthologs in Tfp-expressing gram-positive species that lack an outer membrane (39). Nevertheless, in gram-negative species, PilMNOP also plays an aligning role via the interaction of PilP with the secretin (29, 40). Our findings illustrate the following series of events leading to filament assembly (Fig. 7). PilE subunits are first processed by the prepilin peptidase PilD (8), and accumulate in the cytoplasmic membrane. Importantly, processing in this study was only seen in the presence of PilD, indicating that there was no interference of the prepilin peptidase activity previously reported in a laboratory strain of *E. coli*, which was due to the product of the cryptic *pppA* gene (41). Mature PilE is then "loaded" on the membrane-embedded assembly subcomplex, composed of PilGMNOP, which is powered by the filament extension motor PilF. The role of PilGMNOP would thus be to translate the mechanical energy generated by motion of domains within PilF (13, 42) to pilins, which are simultaneously extruded from the membrane and polymerized into the base of a growing filament (Fig. 7). The wide conservation of the above components (1) suggests that this scenario for filament assembly is broadly applicable.

The other major finding in this study is that native membrane-embedded macromolecular complexes of Pil proteins can be purified, which provides a clearer topological picture of the Tfp assembly machinery (Fig. 7). Purification of PilMNOP as a homogeneous species shows that these four proteins can form a stable subcomplex in the absence of other Pil proteins, with a probable 1:1:1:1 stoichiometry. The findings that PilM, which is

the only cytoplasmic component, is dispensable for complex assembly/stability (PilNOP is very stable), whereas PilP is essential (PilMNO is unstable), are in agreement with previous genetic studies characterizing binary interactions between these proteins (23, 27, 30, 31). The finding that only a small N-terminal portion of PilP, which was shown to interact with PilNO (29), is sufficient for PilNOP stability suggests that PilP plays an indirect role in filament assembly by stabilizing the PilNO heterodimer (24, 26). Curiously, unlike PilMNOP, PilNOP adopts a likely 3:3:3 stoichiometry, which suggests that it is a highly dynamic macromolecular assembly. PilM, which interacts with the cytoplasmic N-terminal portion of PilN (25, 27, 29) and forms a cytoplasmic ring in Tfp subtomograms (34), is thus a peripheral component of the PilMNOP complex, probably recruited to the cytoplasmic membrane once PilNOP is preassembled. Purification of stable PilGMNOP and PilFMNOP complexes confirms that the extension ATPase and platform protein are integral components of the assembly machinery (Fig. 7). PilG is likely to become a stable part of the machinery once PilM has been recruited to the PilNOP complex (PilG does not form a stable complex with PilNOP), which is consistent with Tfp subtomograms showing that the PilG "dome" structure requires the presence of the PilM ring (34). Similarly, the ATPase PilF is likely to be recruited to the complex via interactions with PilM (PilF does not copurify with PilNOP) (33, 43) and/or PilG (32), which is consistent with Tfp subtomograms where the PilF "disc" requires both the PilM ring and PilG dome (34). Finally, PilE from a pool of processed subunits awaiting in the membrane would diffuse to the PilFGMNOP complex (28), which would scoop them out of the lipid bilayer and into the base of a growing filament (Fig. 7).

In conclusion, we provide here an integrated molecular view of the functioning of the machinery involved in the assembly of a filamentous polymer composed of type IV pilins. This provides a layout for the understanding of current and past findings in the field and paves the way for structural analysis of the macromolecular
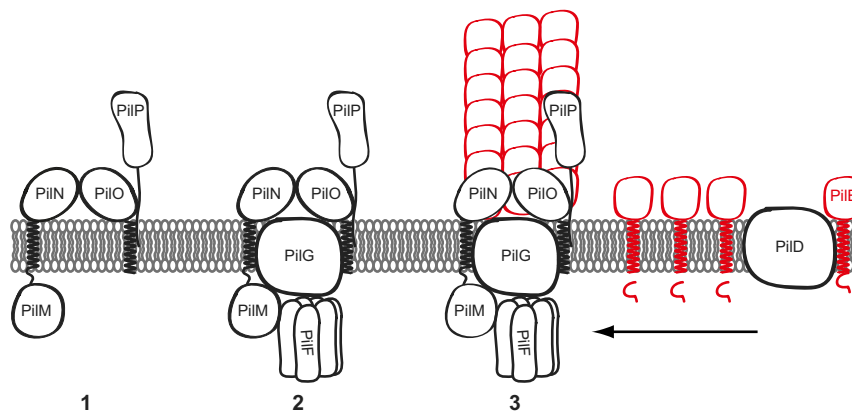
Fig. 7. Working model for the functioning of the minimal machinery capable of building Tfp. 1: The PilMNOP complex is formed. PilM is likely to be recruited to the cytoplasmic membrane upon PilNOP preassembly. 2: The extension ATPase (PilF) and platform protein (PilG) are recruited to the PilMNOP complex, forming the filament assembly machinery. 3: PilE subunits awaiting in the membrane, from a pool of pilins processed by PilD, diffuse to the PilFGMNOP complex, which scoops subunits out of the lipid bilayer and into the base of a growing filament.

complex involved, which suggests that an atomic-level understanding of Tfp assembly is achievable.

Materials and Methods

Bacterial Strains and Plasmids. The *N. meningitidis* strains used in this study were all derived from the sequenced serogroup C clinical isolate 8013 (35). *N. meningitidis* was grown on GC medium base (GCB) agar plates (Difco) containing Kellogg's supplements and, when required, 100 μg/mL kanamycin and 3 μg/mL erythromycin. Plates were incubated in a moist atmosphere containing 5% CO_2. The *pil* mutants used were described in earlier studies (21) or constructed by splicing PCR as described elsewhere (27) using the primers listed in Table S2.

E. coli DH5α was used for cloning experiments in pET-29b (Novagen), whereas cloning in pBAD18 was performed in *E. coli* TOP10 (Invitrogen). Cells were grown in liquid or solid lysogenic broth (LB) (Difco) or LBG (LB supplemented with 1% glucose) either at 37 or 30 °C. When appropriate, the following antibiotics were used: ampicillin 100 μg/mL, chloramphenicol 34 μg/mL, and kanamycin 50 μg/mL. Chemically competent cells were prepared using standard molecular biology techniques. For filament detection and immunoblot analyses, TOP10 cells transformed with pBAD18-borne *pil* operons were grown overnight in LBG at 30 °C in the presence of the relevant antibiotic. Bacteria were reinoculated (1/100) in Terrific Broth supplemented with 1% glucose and without antibiotics, and grown at 30 °C to late exponential phase. Gene expression was then induced with 0.5% arabinose for 1 h before bacteria were placed on ice. Aliquots of each sample were taken for immunoblots and/or IF.

The *pil* operons were constructed as follows using synthetic genes codon-optimized for expression in *E. coli* generated by GeneArt. The plasmids used in this study are listed in Table S3. Genes *pilD*, *pilE*, *pilF*, and *pilG* were synthesized separately, whereas *pilM*, *pilN*, *pilO*, and *pilP* were synthesized as an operon where the last three genes were each preceded by a canonical RBS. Each synthetic gene/group of genes was preceded by a unique NdeI site (CATATG, in which the ATG is the start codon of the gene) and followed by consecutive and unique NheI and XhoI sites (right after the stop codon of the last gene). To construct the various operons, each gene/group of genes extracted as an NdeI and XhoI fragment was subcloned into pET-29b cut with the same enzymes. Then, genes were combined into operons of increasing size using an iterative cloning approach (36). In brief, gene B is extracted from the pET-derived plasmid together with its RBS on an XbaI-XhoI fragment, and cloned into NheI-XhoI immediately downstream of gene A (XbaI and NheI generate compatible cohesive ends). This effectively creates an artificial AB operon whose expression is driven by the T7 promoter. Because the NheI site downstream of gene A is destroyed during this cloning step, the strategy can be used iteratively to create operons of increasing size. Using this methodology, multiple variations of pET29-based operons were generated, numbering up to seven *pil* genes. Toxicity/plasmid instability with pET29-based plasmids prompted us to subclone the above operons into the arabinose-inducible pBAD18 (32). Genes or groups of genes were extracted from pET-29 derivatives on an XbaI-XmaI fragment and subcloned into pBAD18 cut with NheI and XmaI. This effectively placed these genes/operons under the control of the arabinose-inducible promoter in pBAD18.

Because it was impossible to combine all eight *pil* genes in a single operon, we used an alternative cloning strategy to coexpress the corresponding proteins in *E. coli*. We noticed, serendipitously, that *pil* operons subcloned into pBAD18 in the reverse direction of the arabinose-inducible promoter were efficiently expressed from an endogenous σ70 promoter, which we have mapped (Fig. S2). We therefore cloned the *pilDFGE* and *pilDFMNOPE* operons under the control of that σ70 promoter by extracting them from pET-29 derivatives on an XbaI-XmaI fragment and subcloning in pBAD18 cut with the same enzymes. Finally, the missing assembly *pil* genes were subcloned into these plasmids, which were cut by NheI, as XbaI-NheI fragments extracted from pET-29 derivatives. This placed them under the arabinose-inducible promoter, in the reverse direction of the *pil* genes under the σ70 promoter.

E. coli BL21 Star (DE3) (Thermo Fisher Scientific) was used for heterologous expression of full-length native complexes of Pil proteins. Transformed cells were grown in 3 to 12 L of LB at 37 °C, under 180 rpm agitation, until OD_{660} reached 0.6 and then cooled down to 16 °C for 30 min, before inducing overnight with 200 μg/L of anhydrotetracycline (ATc) (IBA). Cells were harvested the next day by centrifuging at 5,000 × *g* at 4 °C for 30 min, and resuspended in buffer (20 mM Tris·HCl, pH 7.5, 100 mM NaCl, 1 mM EDTA) before being flash-frozen in liquid nitrogen and stored at −80 °C.

Plasmids for coexpression and purification of full-length native Pil protein complexes were constructed by subcloning the above *pil* operons into the pASK-IBA3C (IBA) vector, which puts them under an ATc-inducible promoter and fuses a *Strep* tag to the C terminus of the last protein encoded. Initially, the *pilMNOP* operon was cloned into the two BsaI sites in pASK-IBA3C. Addition of *pil* genes with a His tag, as well as deletion or truncation of *pil* genes, was performed using the pASK-*pilMNOP*Strep construct with the In-Fusion Cloning Kit (Clontech).

Purification of Native Membrane-Embedded Macromolecular Complexes. Deep-frozen cell pellets were thawed on ice and incubated for 30 min at 4 °C, under constant agitation (100 rpm), upon addition of lysozyme (1 mg/mL), 1 mM $MgCl_2$, and 5 U benzonase (EMD Millipore). Cell lysis was performed with the EmulsiFlex-C5 homogenizer (Avestin), used at 750 to 1,000 psi. Cell debris was pelleted by centrifugation at 34,000 × *g* for 30 min at 4 °C, before the whole-membrane fraction was pelleted at 112,000 × *g* for 90 min at 4 °C. Cell membranes were resuspended in 20 mM Tris·HCl (pH 7.5) buffer containing 1 mM EDTA and 100 to 250 mM NaCl (depending on the Pil macromolecular complex studied). Membrane proteins were solubilized by adding 1% (wt/vol) β-DDM (Anatrace) detergent to this suspension and stirring at 100 rpm for 1 h at 4 °C. Remaining cell debris was pelleted by centrifugation for 20 min at 112,000 × *g* at 4 °C. The solubilized membrane protein extract was then loaded onto a 5-mL StrepTrap HP affinity column (GE Healthcare) and the Pil multiprotein complexes were pulled down using the C-terminal Strep tag on one of the proteins. In some cases, a second pull-down purification was done using an additional C-terminal His tag on a different protein. Finally, complexes were purified by SEC using HiLoad Superose 6 XK 16/70 PG or 16/600 Superdex 200 PG columns (both from GE Healthcare), depending on the molecular weight of the complex. When the protein yields obtained after the initial affinity-purification step were low,

analytical Superose 6 Increase 10/300 GL or Superdex 200 Increase 10/300 GL columns (both from GE Healthcare) were used instead. Throughout the entire purification, performed at 4 °C, identical buffer conditions were used (20 mM Tris·HCl, pH 7.5, 100 to 250 mM NaCl, 1 mM EDTA, 0.05% β-DDM).

MALDI-TOF and SEC-MALS Analysis of Macromolecular Complexes. Absolute molecular weights of purified PilMOP$_{Strep}$ and PilNOP$_{Strep}$ complexes were determined by SEC-MALS as follows. Protein samples (100 μL at 1 mg/mL in 20 mM Tris·HCl, pH 7.5, 150 mM NaCl, 1 mM EDTA, 0.05% β-DDM) were loaded onto a Superose 6 Increase 10/300 GL column at 0.5 mL/min using an Agilent 1100 series HPLC (Agilent). The column output was fed into a DAWN HELEOS II MALS detector (Wyatt Technology) followed by an Optilab T-rEX differential refractometer (Wyatt Technology), which measures absolute and differential refractive indexes. Data were collected and analyzed using Astra 6.1.2 software (Wyatt Technology). Molecular weights were calculated across eluted protein peaks through extrapolation from Zimm plots using refractive index increment (dn/dc) values of 0.185 mL/g for the protein fraction and 0.1435 mL/g for β-DDM. Three repeat runs were performed for both PilNOP$_{Strep}$ and PilMNOP$_{Strep}$ complexes under identical experimental conditions.

MALDI-TOF MS analysis of the PilMNOP$_{Strep}$ complex in solution was performed at the Max Planck Institute of Biophysics.

SDS/PAGE and Immunoblotting. Whole-cell protein extracts were prepared as previously described for *N. meningitidis* (44), or by resuspending *E. coli* cells directly in Laemmli sample buffer (Bio-Rad) and heating 5 to 10 min at 95 °C. When needed, proteins were quantified using the Bio-Rad Protein Assay as suggested by the manufacturer. Separation of the proteins by SDS/PAGE and subsequent blotting to Amersham Hybond ECL membranes (GE Healthcare) was carried out using standard molecular biology techniques. Blocking overnight (in PBS with 0.5% milk), incubation with primary and/or secondary antibodies (60 min each), and detection using Amersham ECL Plus (GE Healthcare) were carried out following the manufacturer's instructions. Primary antisera were used at 1/100,000 (anti-PilP) or 1/10,000 (anti-PilE, anti-PilF, anti-PilG, anti-PilM, anti-PilN, and anti-PilO). Amersham ECL HRP-linked secondary antibody (GE Healthcare) was used at a 1/10,000 dilution. Blots were imaged with a Bio-Rad ChemiDoc Touch Imaging System.

Tfp Immunodetection. Bacteria were spotted and dried into the wells of a microscope glass slide, fixed with 2.5% paraformaldehyde (in PBS) for 20 min, and quenched with 0.1 M glycine (in PBS) for 5 min. After blocking with 5% milk (in PBS) for 30 min, the monoclonal anti-Tfp 20D9 mouse antibody (1/2,000 in blocking solution) was added and incubated for 30 min. After washing the slides with PBS, cells were stained with DAPI (Thermo Fisher Scientific), whereas Tfp were labeled with a goat anti-mouse antibody coupled to Alexa Fluor 488 (Thermo Fisher Scientific), both added at 1/1,000 dilution (in PBS). After a 30-min incubation and a PBS wash, a coverslip was mounted using Aqua-Poly/Mount (Polysciences). After overnight incubation at 4 °C, samples were viewed and photographed using an Axio Imager A2 microscope (Zeiss). When indicated, cells were submitted to a cold osmotic shock treatment prior to spotting on slides. Four milliliters of culture was centrifuged at 1,200 × *g* for 10 min at 4 °C, and resuspended in 300 μL osmotic buffer (0.1 M Tris acetate, pH 8.2, 0.5 M sucrose, 5 mM EDTA). Lysozyme at 0.1 mg/mL was then added, and samples were left on ice for 5 min. Cells were osmotically shocked and filaments were released by adding 18 mM MgSO$_4$.

RNA Extraction and 5′ RACE. RNA was extracted from *E. coli* cultures grown in LBG to late exponential phase. RNA was extracted using a PureLink RNA Mini Kit (Ambion Life Technologies) and stabilized with RNAprotect Cell Reagent (Qiagen). Transcription start site mapping was done using the 5′ RACE system for rapid amplification of cDNA ends (Invitrogen), according to the manufacturer's instructions.

1. Berry JL, Pelicic V (2015) Exceptionally widespread nanomachines composed of type IV pilins: The prokaryotic Swiss Army knives. *FEMS Microbiol Rev* 39:134–154.
2. Szabó Z, et al. (2007) Identification of diverse archaeal proteins with class III signal peptides cleaved by distinct archaeal prepilin peptidases. *J Bacteriol* 189:772–778.
3. Giltner CL, Nguyen Y, Burrows LL (2012) Type IV pilin proteins: Versatile molecular modules. *Microbiol Mol Biol Rev* 76:740–772.
4. Francetic O, Buddelmeijer N, Lewenza S, Kumamoto CA, Pugsley AP (2007) Signal recognition particle-dependent inner membrane targeting of the PulG pseudopilin component of a type II secretion system. *J Bacteriol* 189:1783–1793.
5. Arts J, van Boxtel R, Filloux A, Tommassen J, Koster M (2007) Export of the pseudopilin XcpT of the *Pseudomonas aeruginosa* type II secretion system via the signal recognition particle-Sec pathway. *J Bacteriol* 189:2069–2076.
6. LaPointe CF, Taylor RK (2000) The type 4 prepilin peptidases comprise a novel family of aspartic acid proteases. *J Biol Chem* 275:1502–1510.
7. Hu J, Xue Y, Lee S, Ha Y (2011) The crystal structure of GXGD membrane protease FlaK. *Nature* 475:528–531.
8. Aly KA, et al. (2013) Cell-free production of integral membrane aspartic acid proteases reveals zinc-dependent methyltransferase activity of the *Pseudomonas aeruginosa* prepilin peptidase PilD. *MicrobiologyOpen* 2:94–104.
9. Kolappan S, et al. (2016) Structure of the *Neisseria meningitidis* type IV pilus. *Nat Commun* 7:13015.
10. Korotkov KV, Gonen T, Hol WG (2011) Secretins: Dynamic channels for protein transport across membranes. *Trends Biochem Sci* 36:433–443.
11. Yamagata A, Tainer JA (2007) Hexameric structures of the archaeal secretion ATPase GspE and implications for a universal secretion mechanism. *EMBO J* 26:878–890.
12. Lu C, Korotkov KV, Hol WG (2014) Crystal structure of the full-length ATPase GspE from the *Vibrio vulnificus* type II secretion system in complex with the cytoplasmic domain of GspL. *J Struct Biol* 187:223–235.
13. Reindl S, et al. (2013) Insights into FlaI functions in archaeal motor assembly and motility from structures, conformations, and genetics. *Mol Cell* 49:1069–1082.
14. Merz AJ, So M, Sheetz MP (2000) Pilus retraction powers bacterial twitching motility. *Nature* 407:98–102.
15. Wolfgang M, Park HS, Hayes SF, van Putten JP, Koomey M (1998) Suppression of an absolute defect in type IV pilus biogenesis by loss-of-function mutations in *pilT*, a twitching motility gene in *Neisseria gonorrhoeae*. *Proc Natl Acad Sci USA* 95:14973–14978.
16. Carbonnelle E, Helaine S, Nassif X, Pelicic V (2006) A systematic genetic analysis in *Neisseria meningitidis* defines the Pil proteins required for assembly, functionality, stabilization and export of type IV pili. *Mol Microbiol* 61:1510–1522.
17. Giltner CL, Habash M, Burrows LL (2010) *Pseudomonas aeruginosa* minor pilins are incorporated into type IV pili. *J Mol Biol* 398:444–461.
18. Winther-Larsen HC, et al. (2005) A conserved set of pilin-like molecules controls type IV pilus dynamics and organelle-associated functions in *Neisseria gonorrhoeae*. *Mol Microbiol* 56:903–917.
19. Wolfgang M, van Putten JP, Hayes SF, Dorward D, Koomey M (2000) Components and dynamics of fiber formation define a ubiquitous biogenesis pathway for bacterial pili. *EMBO J* 19:6408–6418.
20. Koo J, et al. (2008) PilF is an outer membrane lipoprotein required for multi-merization of the *Pseudomonas aeruginosa* type IV pilus secretin. *J Bacteriol* 190:6961–6969.
21. Carbonnelle E, Hélaine S, Prouvensier L, Nassif X, Pelicic V (2005) Type IV pilus biogenesis in *Neisseria meningitidis*: PilW is involved in a step occurring after pilus assembly, essential for fibre stability and function. *Mol Microbiol* 55:54–64.
22. Takhar HK, Kemp K, Kim M, Howell PL, Burrows LL (2013) The platform protein is essential for type IV pilus biogenesis. *J Biol Chem* 288:9721–9728.
23. Ayers M, et al. (2009) PilM/N/O/P proteins form an inner membrane complex that affects the stability of the *Pseudomonas aeruginosa* type IV pilus secretin. *J Mol Biol* 394:128–142.
24. Sampaleanu LM, et al. (2009) Periplasmic domains of *Pseudomonas aeruginosa* PilN and PilO form a stable heterodimeric complex. *J Mol Biol* 394:143–159.
25. Karuppiah V, Derrick JP (2011) Structure of the PilM-PilN inner membrane type IV pilus biogenesis complex from *Thermus thermophilus*. *J Biol Chem* 286:24434–24442.
26. Tammam S, et al. (2011) Characterization of the PilN, PilO and PilP type IVa pilus subcomplex. *Mol Microbiol* 82:1496–1514.
27. Georgiadou M, Castagnini M, Karimova G, Ladant D, Pelicic V (2012) Large-scale study of the interactions between proteins involved in type IV pilus biology in *Neisseria meningitidis*: Characterization of a subcomplex involved in pilus assembly. *Mol Microbiol* 84:857–873.
28. Karuppiah V, Collins RF, Thistlethwaite A, Gao Y, Derrick JP (2013) Structure and assembly of an inner membrane platform for initiation of type IV pilus biogenesis. *Proc Natl Acad Sci USA* 110:E4638–E4647.
29. Tammam S, et al. (2013) PilMNOPQ from the *Pseudomonas aeruginosa* type IV pilus system form a transenvelope protein interaction network that interacts with PilA. *J Bacteriol* 195:2126–2135.
30. Li C, Wallace RA, Black WP, Li YZ, Yang Z (2013) Type IV pilus proteins form an integrated structure extending from the cytoplasm to the outer membrane. *PLoS One* 8:e70144.
31. Friedrich C, Bulyha I, Søgaard-Andersen L (2014) Outside-in assembly pathway of the type IV pilus system in *Myxococcus xanthus*. *J Bacteriol* 196:378–390.
32. Bischof LF, Friedrich C, Harms A, Søgaard-Andersen L, van der Does C (2016) The type IV pilus assembly ATPase PilB of *Myxococcus xanthus* interacts with the inner membrane platform protein PilC and the nucleotide-binding protein PilM. *J Biol Chem* 291:6946–6957.

33. McCallum M, et al. (2016) PilN binding modulates the structure and binding partners of the *Pseudomonas aeruginosa* type IVa pilus protein PilM. *J Biol Chem* 291: 11003–11015.

34. Chang YW, et al. (2016) Architecture of the type IVa pilus machine. *Science* 351: aad2001.

35. Rusniok C, et al. (2009) NeMeSys: A biological resource for narrowing the gap between sequence and function in the human pathogen *Neisseria meningitidis*. *Genome Biol* 10:R110.

36. McLaughlin LS (2013) Heterologous expression of the type IV pilus assembly complex. PhD dissertation (University of Wisconsin–Madison, Madison, WI).

37. Guzman LM, Belin D, Carson MJ, Beckwith J (1995) Tight regulation, modulation, and high-level expression by vectors containing the arabinose PBAD promoter. *J Bacteriol* 177:4121–4130.

38. Pujol C, Eugène E, de Saint Martin L, Nassif X (1997) Interaction of *Neisseria meningitidis* with a polarized monolayer of epithelial cells. *Infect Immun* 65:4836–4842.

39. Gurung I, et al. (2016) Functional analysis of an unusual type IV pilus in the gram-positive *Streptococcus sanguinis*. *Mol Microbiol* 99:380–392.

40. Balasingham SV, et al. (2007) Interactions between the lipoprotein PilP and the secretin PilQ in *Neisseria meningitidis*. *J Bacteriol* 189:5716–5727.

41. Francetić O, Lory S, Pugsley AP (1998) A second prepilin peptidase gene in *Escherichia coli* K-12. *Mol Microbiol* 27:763–775.

42. Mancl JM, Black WP, Robinson H, Yang Z, Schubot FD (2016) Crystal structure of a type IV pilus assembly ATPase: Insights into the molecular mechanism of PilB from *Thermus thermophilus*. *Structure* 24:1886–1897.

43. Sandkvist M, Bagdasarian M, Howard SP, DiRita VJ (1995) Interaction between the autokinase EpsE and EpsL in the cytoplasmic membrane is required for extracellular secretion in *Vibrio cholerae*. *EMBO J* 14:1664–1673.

44. Hélaine S, et al. (2005) PilX, a pilus-associated protein essential for bacterial aggregation, is a key to pilus-facilitated attachment of *Neisseria meningitidis* to human cells. *Mol Microbiol* 55:65–77.